JBC Papers in Press. Published on August 21, 2006 as Manuscript M606360200
The latest version is at http://www.jbc.org/cgi/doi/10.1074/jbc.M606360200

Cyanobacterial Small Chlorophyll Binding Protein ScpD (HliB) Is Located on the Periphery of Photosystem II in the Vicinity of PsbH and CP47 Subunits

Kamoltip Promnares[1,2,3], Josef Komenda[2,3], Ladislav Bumba[4,5], Jana Nebesarova[6], Frantisek Vacha[1,2,4] and Martin Tichy[2,3]

From the [1]Faculty of Biological Sciences, University of South Bohemia, 370 05 Ceske Budejovice, Czech Republic, [2]Institute of Physical Biology, University of South Bohemia, 373 33 Nové Hrady, Czech Republic, [3]Laboratory of Photosynthesis, Institute of Microbiology, Czech Academy of Sciences, 379 81 Trebon, Czech Republic, [4]Institute of Plant and Molecular Biology, Czech Academy of Sciences, 370 05 Ceske Budejovice, Czech Republic, [5]Institute of Microbiology, Czech Academy of Sciences, 142 20, Prague, Czech Republic and [6]Institute of Parasitology, Czech Academy of Sciences, 370 05 Ceske Budejovice, Czech Republic

Running title: Localization of the CAB-like protein

Address correspondence to : Martin Tichy, Institute of Microbiology, Laboratory of Photosynthesis, Opatovicky mlyn, 379 81 Trebon, Czech Republic, Tel. +420-384-722 268; Fax. +420-384-721 246; E-mail: tichym@alga.cz

Cyanobacteria contain several genes coding for small one-helix proteins called SCPs or HLIPs with significant sequence similarity to chlorophyll *a/b*-binding proteins. To localize one of these proteins ScpD in the cells of the cyanobacterium *Synechocystis* sp. PCC 6803, we constructed several mutants in which ScpD was expressed as a His-tagged protein (ScpDHis). Using 2D native-SDS electrophoresis of thylakoid membranes or isolated Photosystem II (PSII), we determined that after high light treatment most of the ScpDHis protein in a cell is associated with PSII. The ScpDHis protein was present in both monomeric and dimeric PSII core complexes and also in the core subcomplex lacking CP43. However, the association with PSII was abolished in the mutant lacking the PSII subunit PsbH. In a PSII mutant lacking cytochrome b_{559}, which does not accumulate PSII, ScpDHis is associated with CP47. The interaction of ScpDHis with PsbH and CP47 was further confirmed by electron microscopy of PSII labeled with Ni-NTA Nanogold. Single particle image analysis identified the location of the labeled ScpDHis at the periphery of the PSII core complex in the vicinity of the PsbH and CP47. Due to the fact that ScpDHis did not form any large structures bound to PSII and due to its accumulation in PSII subcomplexes containing CP47 and PsbH we suggest that ScpD is involved in a process of PSII assembly/ repair during the turnover of pigment-binding proteins, particularly CP47.

Cyanobacteria contain water-soluble peripheral phycobilisomes as their light-harvesting complexes attached to photosystems (1). In higher plants, the same role is played by integral membrane light-harvesting complexes (LHC) composed primarily of LHC proteins containing three transmembrane α-helices and binding chlorophyll (Chl) *a* and *b* (2-5). The sequences of helix I and III are highly similar and evolutionarily-related, comprising the Chl *a/b*-binding (CAB) residues and held together by an arginine (Arg)-glutamic acid (Glu) salt bridge. The CAB residues are made up of about 25 amino acids and include the Chl binding fold. An array of 8 Chl *a*, 6 Chl *b*, 3-4 carotenoids and two lipids are assumed to be bound to each individual LHC apoprotein molecule (6).

LHC proteins are the most abundant members of the extended protein family with conserved Chl-binding residues. Several distant relatives of LHC proteins from this family have been described from higher plants, algae, or cyanobacteria (7). These usually transiently-expressed proteins include the PSII-S protein (4,5,8), one-helix protein or OHP (9), the early light-induced proteins or ELIPs (10,11) and the small cyanobacterial CAB-like proteins or SCPs, also called HLIPs (12,13).

SCPs, predicted to have a single membrane-spanning α-helix, with homologues in red algae and in higher plants, were first identified in the cyanobacterium *Synechococcus elongatus* PCC 7942 (13). *Scp* genes are present in all sequenced cyanobacteria, the highest number of *scp* genes has been found in the genomes of marine cyanobacteria adapted to high light (HL) (14). In the cyanobacterium *Synechocystis* sp. PCC 6803 (hereafter *Synechocystis* 6803) four SCPs have been identified (ScpB-E corresponding to HliC, HliA, HliB, and HliD in (15)). SCPs have been found to be synthesized in response to excess excitation energy stress such as chilling, nitrogen or sulfur deprivation as well as HL (15). Furthermore, the presence of photosynthetic electron transport inhibitor DBMIB, low-intensity blue or UV-A light also induced *scp* genes (16,17). Extensive DNA microarray data confirm that *scp* genes are expressed under various stress conditions, such as: HL, low temperature, hyperosmotic stress, salt stress or the presence of inhibitors of photosynthetic electron transport (18-22). Recent studies suggest that a sensory histidine kinase NblS of *Synechococcus* sp. PCC 7942 may regulate the expression of *scp* genes (23). Moreover, the NblS homologue in *Synechocystis* 6803, Hik33 (also called DspA), also controls the expression of *scp* genes in response to low temperature and osmotic stress (20,24).

Interestingly, the expression of *scp* genes is strikingly similar to that of *Elip* genes (13,15,25) with transient mRNA accumulation during exposure of a plant to a variety of stress conditions that result in the absorption of excess excitation energy (26-28). The ELIPs have been indicated to function in photoprotection (26), most likely by functioning as transient pigment carriers during light-stress-induced turnover of Chl binding proteins (29). Like the ELIPs, the SCPs are localized in the thylakoid membranes and are important for photoacclimation during HL exposure (15,30). By analogy to ELIPs, it has been proposed that SCPs may function directly or indirectly in the dissipation of excess light energy (25,30,31). They could also serve as transient carriers of Chl (12) and modulate tetrapyrrole biosynthesis (32,33). All light-stress-induced LHC relatives from plants studied so far have been found to be associated with photosystems (8,34-36).

Here we demonstrate that the ScpD protein tagged by the His_6 epitope is specifically associated with PSII. Immunogold labeling, followed by single particle analysis, identified the location of the ScpD protein to be at the periphery of the PSII complex. With the help of various PSII mutants, we have shown that ScpD protein interacts with the PSII proteins PsbH and CP47. These results are discussed in terms of the ScpD role in PSII.

EXPERIMENTAL PROCEDURES

Growth Conditions - Wild type (WT) and mutants (as described in Table I) of *Synechocystis* 6803 were grown in liquid BG-11 medium (37) supplemented by 10 mM glucose at 30°C at 30 μmol m^{-2} s^{-1} (in PSI containing strain) or 3 μmol m^{-2} s^{-1} (in PSI^- strain) on a rotary shaker. For HL treatment, cells were incubated at 500 μmol m^{-2} s^{-1}. *Mutant Construction* - The *Synechocystis* 6803 ScpDHis strain with ScpD protein tagged with the His_6 epitope (His tag) on its N-terminus, expressed under *psbA2* promoter, was constructed in a procedure analogous to that described in (38). The *scpD* gene was amplified by PCR using a mix of *Taq* and *Pfu* DNA polymerases and gene specific primers with artificially-generated restriction sites for *Nde*I and *Bam*HI and containing 6 histidine codons (CAT) in the forward primer. After restriction, the PCR fragment was cloned into the *Nde*I and *Bam*HI sites of the pSBA plasmid (39) containing the upstream and downstream regions of the *Synechocystis* 6803 *psbA2* gene. The ligation mix was amplified by PCR using pSBA primers amplifying the *scpDHis* gene flanked by 0.5 kbp upstream and downstream regions of *psbA2*. This 1.2 kbp PCR product was directly used to transform the *Synechocystis* 6803 *psbAII*-KS strain, where the *psbA2* gene was replaced by a kanamycin-resistance/*sacB* cartridge (39). The *sacB* gene codes for levan sucrase, leading to sucrose sensitivity of this strain. After transformation, *Synechocystis* cells were grown on BG-11 plates for 4 days. The transformants were then transferred to plates with 5% sucrose and sucrose-resistant colonies were checked for kanamycin sensitivity. The resulting strain expressing both the wild type and His tagged forms of ScpD protein was transformed with chromosomal DNA from the ΔScpD strain (32).

Proper insertion of the *scpDHis* gene was confirmed by DNA sequencing, and deletion of the WT copy of the *scpD* gene was confirmed by PCR.

The ScpDHis/ΔScpD strain was transformed with chromosomal DNA from a PSI^- cell to obtain the ScpDHis/ΔScpD/PSI^- strain. The ScpDHis/ΔScpD/PSI^- strain was further transformed with chromosomal DNA from ΔCyt, ΔCP47, and ΔH cells (see Table I). The deletions were confirmed by PCR.

Radiolabeling of the Cells, Membrane Preparation and Protein Analysis Using 2D-Blue Native/SDS, 2D-Native Deriphat/SDS Electrophoresis and Immunoblotting - Radioactive labeling of cells using a mixture of L-[^{35}S]-methionine and L-[^{35}S]-cysteine (>1000 Ci mmol^{-1}, Trans-label, ICN, final activity 400 μCi ml^{-1}) and isolation of membranes was performed as described in (40). Isolated membranes were solubilized with n-dodecyl-β-maltoside (DM) (DM/Chl = 20 and 100 (w/w) in PSI-containing and PSI^- strain, respectively), and obtained complexes were separated in the first dimension by either blue-native electrophoresis at 4ºC in 5-14% polyacrylamide gel according to (41) or native Deriphat electrophoresis as described in (42). Subunit composition of the complexes was assessed by electrophoresis in a denaturing 12-20% linear gradient polyacrylamide gel containing 7 M urea (in the second dimension) (40). Proteins separated in the gel were transferred onto PVDF membrane. The membrane was incubated with specific primary antibodies followed by incubation with a secondary antibody conjugated with horseradish peroxidase (Sigma, USA) and chemiluminescence Lumi-light substrate (Roche, Germany). The primary antibodies used in the study were raised in rabbits against: (i) residues 58-86 of the spinach D1 polypeptide, (ii) residues 380-394 of barley CP47 (40), and (iii) monoclonal anti-polyhistidine (Sigma, USA). For autoradiography, the gel or the membrane with labeled proteins was exposed to X-ray film at laboratory temperature for 2-3 days.

Isolation of PSII and Protein Analysis - The isolation of thylakoid membranes was performed as described in (42). The thylakoid membranes were washed until the supernatant became colorless with a buffer containing 25 mM MES, pH 6.5, 5 mM $MgCl_2$ and 5 mM $CaCl_2$. The washed thylakoid membranes (0.25 mgChl ml^{-1}) were solubilized with DM (1% final concentration) for 10 min on ice. Nonsolubilized material was removed by centrifuging at 18,000 rpm for 10 min at 4ºC. PSII complexes were either isolated using sucrose density-gradient centrifugation or a combination of affinity and anion exchange chromatography. The supernatant was loaded onto a discontinuous sucrose gradient (20, 30 and 50%, respectively) in buffer containing 25 mM MES, pH 6.5, 5 mM $MgCl_2$, 5 mM $CaCl_2$ and 0.04% DM. The PSII complexes were separated by centrifugation at 100,000 rpm (HITACHI Himac CS 120 FX, S100AT5-0208 rotor) for 4 h at 4ºC. The monomeric and dimeric PSII was recovered from the sucrose gradient and concentrated on Microcon YM-50. For chromatography, the supernatant was applied onto the column of chelating Sepharose loaded with copper ions and then the non-bound material directly passed onto the Q-Sepharose column (Amersham Pharmacia, Sweden) from which the PSII complexes were eluted by 25 mM MES, pH 6.5 containing 250 mM NaCl and 0.03% DM as described in (42). Composition of isolated PSII was analyzed by SDS-PAGE in a denaturing 12-20% linear gradient polyacrylamide gel containing 7 M urea. For electrophoresis, the isolated PSII was solubilized in 25 mM Tris/HCl, pH 6.8, containing 2% SDS (w/v) and 2% dithiothreitol (w/v) at room temperature for 60 min. Separated proteins in the gel were either stained by Coomassie Blue or transferred onto PVDF membrane and used for immunodetection.

Determination of Chl - Chl was extracted from cell pellets (50 ml, OD_{730} ~ 0.5) by 100% methanol. Chl content was measured spectrophotometrically on a Spectronic Unicam UV500 spectrophotometer (43).

Gold Labeling of the His-tagged PSII Particles - To visualize the position of the ScpDHis subunit, Ni-NTA Nanogold (Nanoprobes Inc, USA) was used. This label is a gold cluster with attached Ni^{2+} enabling specific binding of the gold particle to the His-tagged proteins. Well-washed thylakoid membranes were suspended in a buffer containing 20 mM Tris, pH 7.4, 100 mM NaCl, and 5 mM $CaCl_2$ at a Chl concentration of 100 μg ml^{-1} and mixed with an equal volume of Ni-NTA Nanogold solution (30 nM). The solution was incubated for 30 min at 4°C and the free Ni^{2+}-NTA groups on

gold labels were saturated by 1 mM L-histidine for a further 10 min on ice. Thylakoid membranes were then solubilized with 1% DM for 15 min and the unsolubilized material was removed by centrifugation at 60,000 × *g* for 30 min. The supernatant was loaded onto a freshly prepared 0.1–1.2 M continuous sucrose density gradient prepared by freezing and thawing the centrifuge tubes filled with a buffer containing 20 mM Tris (pH 7.4), 0.6 M sucrose, 10 mM NaCl, 5 mM $CaCl_2$, and 0.05% DM (44) and the PSII complexes were separated by centrifugation at 150,000 × *g* (Hitachi, P56SW rotor) for 14 h at 4°C. The lower green band containing the PSII dimers was harvested with a syringe and loaded onto a Sephadex G-25 (Amersham Biosciences) desalting column equilibrated with 20 mM Tris (pH 7.4) containing 0.05% DM. Non-labeled PSII particles were prepared as described above, but the Ni-NTA Nanogold labeling step was omitted during the procedure.

Electron Microscopy and Image Analysis - Freshly-prepared labeled PSII complexes eluted from the desalting column were placed on glow-discharged carbon-coated copper grids and negatively stained with 0.75% uranyl acetate. Electron microscopy was performed with a Philips TEM 420 electron microscope using 80 kV at 60,000 × magnification. Micrographs free from astigmatism and drift were scanned with a pixel size corresponding to 4.5 Å at the specimen level. Image analyses were carried out using SPIDER software (45). From 63 micrographs of the PSII cores, about 2900 top-view projections of unlabeled particles and 472 side-view projections of labeled particles were selected for analysis. Both separate data sets were rotationally and translationally aligned, and subjected to multivariate statistical analysis in combination with classification (46,47). Classes from each of the subsets were used for refinement of alignments and subsequent classifications. For the final sum, the best of the class members were summed using a cross-correlation coefficient of the alignment procedure as a quality parameter. The resolution of the images was calculated using the Fourier ring correlation method (48). For molecular modeling, the coordinates were taken from the Protein Data Bank (www.rcsb.org/pdb) under the code 1S5L for PSII structure at 3.5 Å resolution (49). The overlay cartoon was generated by the freeware program Accelrys ViewerLite 4.2

RESULTS

ScpDHis Protein Is Localized in the Thylakoid Membrane

To localize the ScpD protein in the cells of *Synechocystis* 6803, we constructed mutants in which the *scpD* gene had been tagged by the His_6 epitope (ScpDHis strains) as described in Material and Methods. As higher accumulations of ScpC/D proteins have been detected in PSI^- strains (12), the ScpDHis/ΔScpD/PSI^- strain was used to determine the localization of the ScpDHis protein. Using the anti-His monoclonal antibody, a single band was detected in the thylakoids of the ScpDHis/ΔScpD/PSI^- strain (Fig. 1). No such band was detected in the fraction of soluble proteins from this strain and in the thylakoids of PSI^- (not shown) and ScpDHis/ΔScpD strains grown at 50 µmol m^{-2} s^{-1} (Fig. 1). However, the ScpDHis band was detectable in the ScpDHis/ΔScpD strain grown under HL (Fig. 1).

The ScpDHis Protein Is Associated with Photosystem II

To further localize the ScpDHis protein in the thylakoid membranes, we performed 2D analysis of thylakoid proteins. Mildly solubilized thylakoid protein complexes from the ScpDHis/ΔScpD/PSI^- strain were first separated by non-denaturing blue native (BN) or Deriphat PAGE and their subunit composition was determined by SDS-PAGE in combination with Western blotting in the second dimension. Both methods yielded similar results with the majority of the ScpDHis being present in two complexes at about 300 and 220 kDa (Fig. 2A). These complexes had been previously identified as a monomeric reaction center core complex (RCC1) and a smaller reaction center core subcomplex (RC47), which contains CP47 but no CP43 (40) (Fig. 3). BN-PAGE provided a better separation of the complexes than Deriphat-PAGE (not shown) and was therefore used subsequently. In the ΔCP47 background where no PSII core is assembled, the ScpDHis/ΔScpD/PSI^-/ΔCP47 mutant accumulated a significant amount of ScpDHis; however this protein was localized in a region of the small protein complexes and free

proteins (Fig. 2B). Thus, ScpDHis co-migrated with PSII in two different buffer systems and ScpDHis association with large thylakoid complexes was dependent on PSII accumulation, indicating that ScpDHis is associated with PSII.

To confirm that the ScpDHis protein is indeed associated with PSII we used a combination of several independent methods for isolation of PSII. Monomeric and dimeric reaction center core complexes were isolated from the ScpDHis/ΔScpD/PSI$^-$ strain by sucrose density-gradient centrifugation or by a combination of affinity and ion exchange chromatography. The complexes were further purified by BN-PAGE. Green PSII bands were cut from the native gel and subjected to SDS-PAGE and immunodetected with anti-His antibody. ScpDHis protein was present in all PSII preparations (Fig. 4).

The His tag is widely used to isolate tagged proteins under native conditions by nickel affinity chromatography allowing co-purification of proteins associated with the tagged protein. However, native isolation of the ScpDHis protein was not successful and no ScpDHis protein was found in the fraction eluted from the nickel column (not shown).

ScpDHis Protein Expression

As the ScpDHis protein had been expressed under light-inducible *psbA2* promoter, we tried to follow its expression after HL treatment. Protein expression in WT and ScpDHis/ΔScpD cells was compared using autoradiography after 2D-PAGE (BN/SDS-PAGE). Cells were pulse labeled with a mixture of [^{35}S] Met and Cys under HL conditions. Electrophoretic analysis of labeled proteins and autoradiography showed the expression of a new 7 kDa protein in the ScpDHis/ΔScpD strain that was absent in WT. Again, this protein was associated with RCC1 and RC47 (Fig. 3). The position of this 7 kDa protein on the membrane was identical to that of the ScpDHis protein detected by immunoblotting (Fig. 2A) demonstrating that the expressed protein is ScpDHis.

The ScpDHis Protein Is Associated with CP47 and PsbH

Previous results showed that the ScpDHis protein is associated with PSII. To localize this protein more precisely, we followed the association of ScpDHis with other PSII proteins in several mutants lacking individual PSII subunits. Interestingly, in the ΔH background (strain ScpDHis/ΔScpD/PSI$^-$/ΔH containing ScpDHis but lacking PSI and the PsbH subunit of PSII), the ScpDHis protein was not associated with PSII but was present in a region of small protein complexes or free proteins (Fig. 5). Note that the ΔH mutant grown in the presence of glucose exhibits activity in oxygen evolution similar to that of WT (50) and also contains a similar set of PSII complexes (51). This indicates that the PsbH protein is necessary for ScpDHis association with PSII.

Unlike the ΔH strain, the mutant ΔCyt lacking the *psbEFLJ* operon does not accumulate any stable PSII subcomplexes, however it does contain a small amount of unassembled CP47 that is resolved in the BN gels as a double band (40) containing not only CP47 but also PsbH (51). In the ScpDHis/ΔScpD/PSI$^-$/ΔCyt strain, most of the ScpDHis protein was present in a region of small protein complexes or free proteins (Fig. 5). However, a significant amount of ScpDHis was associated with one of the two bands of unassembled CP47. The observation that ScpD is indeed part of this CP47-PsbH complex and that co-migration with CP47 on a 2D gel (Fig. 5) is not just accidental, was confirmed by isolation of this complex from the ΔCyt strain expressing the His-tagged PsbH (not shown). This indicates that ScpDHis is associated with CP47 and PsbH under conditions when PSII assembly is blocked at the early step of formation of reaction center (RC) complexes due to the absence of cytochrome b_{559} and D2 (40).

Localization of ScpDHis Using Electron Microscopy

To further confirm the location of the His-tagged ScpD subunit within PSII, the dimeric PSII complexes were labeled with Ni-NTA Nanogold and visualized in an electron transmission microscope. As the labeling procedure previously used for the localization of the PsbH protein (52) yielded no labeling, an alternative procedure had to be developed that included direct labeling of thylakoid membranes prior to their solubilization and isolation of PSII complexes.

The electron micrographs revealed that the preparation contained dispersed particles with uniform size and shape and almost free of contaminants. The images contained dimeric PSII particles, mostly in their top-view projections (i.e.

perpendicular to the original membrane plane). Side-view projections were less common and usually occurred as an aggregation of two single PSII complexes attached by their stromal surfaces (Fig. 6). Fig. 6 also shows that not all PSII particles carried gold labels. To localize the gold label within PSII dimers, both labeled and unlabeled particles were extracted from the micrographs, aligned, subjected to multivariate statistical analysis and classified. The most representative class averages of both labeled and unlabeled particles are depicted in Fig. 7. The top-view projections showed diamond-shaped particles with two-fold rotational symmetry around the center of the complex. The class averages closely resembled the PSII dimers without the ScpDHis protein (44,53,54). All the projections had the same type of handedness and no mirror images were detected, thus indicating a preferred orientation of the PSII dimers with their stromal side to the carbon support film. One part of the labeled top views had a gold label only on one side of the complex, whereas another part exhibited gold labels on both sides of the complex (Fig. 7D, E). This indicates the ScpDHis protein as being located on both sides of the complex, reflecting the two-fold rotational symmetry of the dimeric PSII complex.

The side-view projections showed two single PSII dimers aggregated with their stromal surface (Fig. 7C). Protrusions on the lumenal sides of the single PSII dimer corresponded to the proteins of the oxygen-evolving complex (44). In side views the labels were located between the two single PSII particles in the paired structures (Fig. 7F). This clearly identifies the His-tag, and therefore, the N-terminus of the ScpD protein on the stromal side of the PSII complex.

DISCUSSION

We have expressed ScpD as a His-tagged protein on its N-terminus to enable its isolation and localization within the thylakoid membranes. The ScpDHis protein was expressed under *psbA2* promoter. Unlike the native *scpD* promoter, the *psbA2* promoter belongs to those promoters with a high expression level even in low light (55) that is further increased under HL conditions. However, no accumulation of ScpDHis protein was observed in the cells grown in normal light, similar to what was observed for the native ScpD protein (12). This shows that different levels of the *scpDHis* and the *scpD* transcript did not influence the accumulation of both proteins in the cell, indicating that accumulation of ScpD is controlled mostly by other factors. Accordingly, in the PSI$^-$ background, ScpDHis accumulated even under low-light conditions, similar to that observed for the native ScpD (12).

Using several independent methods, we have determined that after HL treatment most of the ScpDHis protein in a cell is associated with PSII. The ScpDHis protein was present in both monomeric and dimeric PSII reaction center core complexes and also in the RC47 subcomplex lacking CP43, indicating that the CP43 subunit is not necessary for the association of ScpDHis with PSII. The specific interaction of ScpDHis with PSII was further confirmed by the observation that in the absence of PSII, the ScpDHis protein was present in the form of small protein complexes. This also indicated that ScpDHis does not interact with other large thylakoid membrane complexes, particularly PSI, as was shown recently for the plant SCP homologue OHP (36). We also succeeded in a more detailed localization of ScpDHis within PSII as we detected the protein in the complex of CP47 and PsbH that accumulates at low levels in the strain unable to assemble PSII complexes due to missing cytochrome b_{559} (Fig. 5). Thus, ScpDHis seems to bind to PSII in proximity to the CP47-PsbH proteins. This corresponds well with the observation that in the strain ΔH lacking the small PsbH protein, ScpDHis is no longer detected within PSII, indicating that the PsbH protein is important for the proper association of ScpDHis with PSII.

The His-tagged ScpD protein, this time with the tag on the C-terminus, has been used previously to follow ScpD accumulation and potential association with other proteins (15). Interestingly, in this study the ScpD protein was found in the ~ 100 kDa fraction after gel filtration, apparently not associated with PSII. This raises the question as to whether the observed association of ScpDHis with PSII is not an artifact caused by the His tag. This is probably not the case as the native forms of ScpD and ScpC seem to be also associated with PSII (see below). We also attempted to isolate complexes containing ScpDHis under native conditions by nickel affinity

chromatography in a similar procedure that we have used recently for the His-tagged PsbH protein (52). However, no ScpDHis protein was found in the fraction eluted from the column. We assume that this may be caused by the low accessibility of the His tag on ScpD bound to the PSII complex.

Similar problems were encountered during labeling of ScpDHis for single particle analysis by Ni-NTA Nanogold, when no label was bound to PSII. Therefore, a different labeling procedure than the one used recently for the His-tagged PsbH protein (52) had to be developed for a successful labeling. The combination of Ni-NTA Nanogold labeling of His-tagged protein and single particle analysis provides an excellent tool to localize protein subunits within a protein complex (52,56). The main advantage to conventional immunogold labeling procedures is the close proximity of the gold particle to the His tag, enabling a more accurate localization of the target protein. Using this procedure we localized the ScpDHis protein on the periphery of PSII dimers. To identify PSII proteins in the vicinity of the gold label we have overlaid a model of the transmembrane helix organization of PSII into a top-view projection map of the labeled PSII particle. Figure 8 shows that the Ni-NTA gold label is found to be close to the transmembrane helices of the CP47 and PsbH proteins. This is in full agreement with other data indicating the proximity of ScpDHis to the CP47 and PsbH proteins. Moreover, the labeling confirmed that the Ni-NTA Nanogold and therefore, also, the N-terminus of the ScpD protein is localized on the stromal side of the thylakoid membrane. Electron microscopy and single particle analysis did not reveal any differences between PSII dimers isolated from normal or HL-treated cells, indicating that SCPs do not form large complexes at or around PSII comparable to IsiA rings formed around the PSI trimers in iron-depleted conditions (57). When compared with the location of the PSII subunit PsbH using a similar approach (52), localization of the gold label on the ScpDHis protein is less distinct (Fig. 7D, E). This may indicate that the position of ScpDHis in PSII is more ambiguous. Moreover, several gold labels were distinguishable on each side of the PSII dimer, indicating that more than one copy of ScpDHis may be bound per PSII monomer.

We believe that the native ScpD protein (without the His tag) is also associated with PSII. On 2D autoradiograms, ScpDHis is identified as a strong 7 kDa band (Fig. 3), the size of the native ScpD being expected to be about 6 kDa. Interestingly, a prominent 6 kDa band is present in WT, with a similar pattern of association with both PSII core complexes as we have shown for ScpDHis (Fig. 3). Moreover, this 6 kDa protein did not associate with PSII in the ΔH background similarly as in the case of ScpDHis (Komenda unpublished). We think that this 6 kDa band in WT is formed at least in part by native ScpD. However, the 6 kDa band is still present in the ScpDHis/ΔScpD mutant lacking the native ScpD protein (Fig. 3). We speculate that this band belongs to the ScpC protein known to have similar electrophoretic mobility as ScpD (15). Indirect evidence indicates that ScpD may associate with the highly homologous ScpC in thylakoid membranes, based on their co-purification during gel filtration of solubilized thylakoids and on their accumulation kinetics following exposure to HL (15). ScpC and ScpD have been also proposed to functionally complement each other (33). SCPs are generally expected to form complexes in the thylakoid membranes based on the presumption that they are Chl-binding proteins and that in LHCII, interaction of two homologous helices is necessary for pigment binding (58). Indeed, SCPs have been detected in high-molecular-weight complexes/aggregates by gel filtration (15) or electrophoresis (12).

ScpD is considered to be a general stress protein that accumulates under various stress conditions. Extensive DNA microarray data show that ScpD is induced by almost all stresses tested including HL, nutrient deprivation or low temperature (18,20,59). In our experiments, ScpD protein became one of the most expressed proteins in the thylakoid membranes after 30 min of HL treatment (Fig. 3). However, *scp* genes are also expressed under standard growth conditions (18-22). In cells maintained in low light and under optimal growth conditions, low levels of SCPs have been detected after partial purification (15).

SCPs and their larger relatives, ELIPs containing three transmembrane helices, share more than just the Chl-binding motif. Both groups exhibit a similar pattern of expression under various stress conditions and both represent

relatively short-lived proteins (11,15). Similarly to the association of ScpDHis with PSII, ELIP in pea has been found in the margins of the grana where PSII is assembled, and cross-linking experiments indicated the proximity of the pea ELIP to PSII (34). Based on these similarities, analogous functions have been proposed for both SCPs and ELIPs, ranging from a transient pigment carrier function (33,60) to their role in the dissipation of excess light energy (30,31). Indirect evidence is growing that ELIPs may be involved in the binding of Chl released during turnover of PSII and in protein stabilization during PSII assembly (29). ELIPs are expressed not only under typical stress conditions represented by HL stress or in the process of thylakoid biogenesis during greening, but also during the reverse process of thylakoid disassembly - represented by leaf senescence (61) or by chloroplast-to-chromoplast transitions during fruit ripening (62). This emphasizes the ubiquity of ELIPs during normal developmental processes when there is an increased pigment/protein turnover. Also SCPs are implicated in several processes involving Chl biosynthesis and/or accumulation. Similar to ELIPs, SCPs are necessary to ensure a high rate of Chl accumulation in cells during greening (33,63). Also Chl stability in the dark was negatively influenced by the absence of SCPs (33). This may be explained by the destabilization of PSII pigment-protein complexes and/or by inefficient Chl recycling (33). This is in line with our observation that ScpD significantly accumulates after several days of incubation in the dark (Promnares unpublished), suggesting that SCPs are physically present there to fulfill the above functions and that accumulation of SCPs can be also triggered by factors other than external stress. Interestingly, CP47, the binding partner of ScpDHis, is the most stable Chl protein of PSII and during PSII assembly and repair it is the most frequently reused large PSII subunit - as demonstrated by significantly lower levels of its radioactive labeling in comparison with D1, D2 and CP43 (40). Thus, it is tempting to speculate that SCPs contribute to this stability of CP47.

In conclusion, we have shown that the His-tagged ScpD protein, an abundant member of the SCP family in *Synechocystis* 6803 is located on the periphery of PSII in the proximity of the PSII subunits CP47 and PsbH. This localization is in accordance with most of the functions suggested for SCPs. However, due to the observed stoichiometry of only one to several copies of ScpD per PSII and due to the ScpD presence in PSII subcomplexes containing CP47 and PsbH we favor the idea of ScpD being involved in the process of stabilization of pigment-binding proteins, particularly CP47, during PSII assembly and repair.

REFERENCES

1. Bryant, D. A. (1991) in *The Photosynthetic Apparatus: Molecular Biology and Operation* (Bogorad, L., and Vasil, I. K., eds), pp. 257-300, Academic Press, San Diego, CA
2. Kühlbrandt, W., Wang, D., and Yoshinori, F. (1994) *Nature* **367**, 614-621
3. Jansson, S. (1994) *Biochim. Biophys. Acta* **1184**, 1-19
4. Kim, S., Sandusky, P., Bowlby, N. R., Aebersold, R., Green, B. R., Vlahakis, S., Yocum, C. F., and Pichersky, E. (1992) *FEBS Lett.* **314**, 67-71
5. Wedel, N., Klein, R., Ljungberg, U., Andersson, B., and Herrmann, R. G. (1992) *FEBS Lett.* **314**, 61-66
6. Standfuss, J., Terwisscha van Scheltinga, A. C., Lamborghini, M., and Kühlbrandt, W. (2005) *EMBO J.* **24**, 919-928
7. Adamska, I. (2001) in *Advances in Photosynthesis and Respiration-Regulation of Photosynthesis* (Aro, E. M., and Andersson, B., eds) Vol. 11, pp. 487-505, Kluwer, Dordrecht, The Netherlands
8. Funk, C., Schröder, W., Napiwotzki, A., Thus, S., Renger, G., and Andersson, B. (1995) *Biochemistry* **34**, 11133-11141
9. Jansson, S. (1999) *Trends Plant Sci.* **4**, 236-240
10. Green, B. R., Pichersky, E., and Kloppstech, K. (1991) *Trends Biochem. Sci.* **16**, 181-186
11. Adamska, I., Ohad, I., and Kloppstech, K. (1992) *Proc. Natl. Acad. Sci. U.S.A.* **89**, 2610-2613
12. Funk, C., and Vermaas, W. (1999) *Biochemistry* **38**, 9397-9404
13. Dolganov, N. A. M., Bhaya, D., and Grossman, A. R. (1995) *Proc. Natl. Acad. Sci. U.S.A.* **92**, 636-640
14. Bhaya, D., Dufresne, A., Vaulot, D., and Grossman, A. R. (2002) *FEMS Microbiol. Lett.* **215**, 209-219
15. He, Q., Dolganov, N., Björkman, O., and Grossman, A. R. (2001) *J. Biol. Chem.* **276**, 306-314
16. Salem, K., and Waasbergen, L. G. v. (2004) *Plant Cell Physiol.* **45**, 651–658
17. Salem, K., and van Waasbergen, L. G. (2004) *J. Bacteriol.* **186**, 1729-1736
18. Hihara, Y., Kamei, A., Kanehisa, M., Kaplan, A., and Ikeuchi, M. (2001) *Plant Cell* **13**, 793–806
19. Allakhverdiev, S. I., Nishiyama, Y., Miyairi, S., Yamamoto, H., Inagaki, N., Kanesaki, Y., and Murata, N. (2002) *Plant Physiol.* **130**, 1443–1453
20. Mikami, K., Kanesaki, Y., Suzuki, I., and Murata, N. (2002) *Mol. Microbiol.* **46**, 905–915
21. Kanesaki, Y., Suzuki, I., Allakhverdiev, S. I., Mikami, K., and Murata, N. (2002) *Biochem. Biophys. Res. Commun.* **290**, 339–348
22. Hihara, Y., Sonoike, K., Kanehisa, M., and Ikeuchi, M. (2003) *J. Bacteriol.* **185**, 1719–1725
23. van Waasbergen, L. G., Dolganov, N., and Grossman, A. R. (2002) *J. Bacteriol.* **184**, 2481-2490
24. Suzuki, I., Kanesaki, Y., Mikami, K., Kanehisa, M., and Murata, N. (2001) *Mol. Microbiol.* **40**, 235-244
25. Jansson, S., Andersson, J., Kim, S. J., and Jackowski, G. (2000) *Plant Mol. Biol.* **42**, 345-351
26. Adamska, I., and Kloppstech, K. (1994) *J. Biol. Chem.* **269**, 30221-30226
27. Montané, M. H., Dreyer, S., Triantaphylides, C., and Kloppstech, K. (1997) *Planta* **201**, 293-301
28. Heddad, M., and Adamska, I. (2000) *Proc. Natl. Acad. Sci. U.S.A.* **97**, 3741-3746
29. Hutin, C., Nussaume, L., Moise, N., Moya, I., Kloppstech, K., and Havaux, M. (2003) *Proc. Natl. Acad. Sci. U.S.A.* **100**, 4921-4926
30. Havaux, M., Guedeney, G., He, Q., and Grossman, A. R. (2003) *Biochim. Biophys. Acta* **1557**, 21-33
31. Montané, M. H., and Kloppstech, K. (2000) *Gene* **258**, 1-8
32. Xu, H., Vavilin, D., Funk, C., and Vermaas, W. (2002) *Plant Mol. Biol.* **49**, 149–160
33. Xu, H., Vavilin, D., Funk, C., and Vermaas, W. (2004) *J. Biol. Chem.* **279**, 27971–27979
34. Adamska, I., and Kloppstech, K. (1991) *Plant Mol. Biol.* **16**, 209-223
35. Levy, H., Gokhman, I., and Zamir, A. (1992) *J. Biol. Chem.* **266**, 13698-13705

36. Andersson, U., Heddad, M., and Adamska, I. (2003) *Plant Physiol.* **132**, 811-820
37. Rippka, R., Deruelles, J., Waterbury, J. B., Herman, M., and Stanier, R. Y. (1979) *J. Gen. Microbiol.* **111**, 1-61
38. Tichý, M. (2003) *Photosynthetica* **41**, 583-588
39. Lagarde, D., Beuf, L., and Vermaas, W. (2000) *Appl. Environ. Microbiol.* **66**, 64-72
40. Komenda, J., Reisinger, V., Müller, B. C., Dobáková, M., Granvog, B., and Eichacker, L. A. (2004) *J. Biol. Chem.* **279**, 48620-48629
41. Schägger, H., and von Jagow, G. (1991) *Anal. Biochem.* **199**, 223-231
42. Komenda, J., Lupínková, L., and Kopecký, J. (2002) *Eur. J. Biochem.* **269**, 610-619
43. Porra, R. J., Thompson, W. A., and Kriedemann, P. E. (1989) *Biochim. Biophys. Acta* **975**, 384-394
44. Bumba, L., Havelkova-Dousova, H., Husak, M., and Vacha, F. (2004) *Eur. J. Biochem.* **271**, 2967-2975
45. Frank, J., Radermacher, M., Penczek, P., Zhu, J., Li, Y. H., Ladjadj, M., and Leith, A. (1996) *J. Struct. Biol.* **116**, 190-199
46. van Heel, M., and Frank, J. (1981) *Ultramicroscopy* **6**, 187-194
47. Harauz, G., Boekema, E., and van Heel, M. (1988) *Methods Enzymol.* **164**, 35-49
48. van Heel, M. (1987) *Ultramicroscopy* **21**, 95-100
49. Ferreira, K. N., Iverson, T. M., Maghlaoui, K., and Barber, J. (2004) *Science* **303**, 1831-1838
50. Mayers, S. R., Dubbs, J. M., Vass, I., Hideg, E., Nagy, L., and Barber, J. (1993) *Biochemistry* **32**, 1454-1465
51. Komenda, J., Tichý, M., and Eichacker, L. A. (2005) *Plant Cell Physiol.* **46**, 1477-1483
52. Bumba, L., Tichy, M., Dobakova, M., Komenda, J., and Vacha, F. (2005) *J. Struct. Biol.* **152**, 28-35
53. Kuhl, H., Rogner, M., van Breemen, J. F. L., and Boekema, E. J. (1999) *Eur. J. Biochem.* **266**, 453-459
54. Nield, J., Kruse, O., Ruprecht, J., da Fonseca, P., Buchel, C., and Barber, J. (2000) *J. Biol. Chem.* **275**, 27940-27946
55. Mohamed, A., Eriksson, J., Osiewacz, H. D., and Jansson, C. (1993) *Mol. Gen. Genet.* **238**, 161-168
56. Buchel, C., Morris, E., Orlova, E., and Barber, J. (2001) *J. Mol. Biol.* **312**, 371-379
57. Bibby, T. S., Nield, J., and Barber, J. (2001) *Nature* **412**, 743-745
58. Ke, B. (2001) in *Photosynthesis: Photobiochemistry and Photobiophysics*, pp. 215-228, Kluwer Academic Publishers, Dordrecht, The Netherlands
59. Singh, A. K., McIntyre, L. M., and Sherman, L. A. (2003) *Plant Physiol.* **132**, 1825–1839
60. Adamska, I. (1997) *Physiol. Plant* **100**, 794-805
61. Binyamin, L., Falah, M., Portnoy, V., Soudry, E., and Gepstein, S. (2001) *Planta* **212**, 591-597
62. Bruno, A. K., and Wetzel, C. M. (2004) *J. Exp. Bot.* **55**, 2541-2548
63. Casazza, A. P., Rossini, S., Rosso, M. G., and Soave, C. (2005) *Plant Mol. Biol.* **58**, 41-51
64. Williams, J. G. (1988) *Methods Enzymol.* **167**, 766-778
65. Pakrasi, H. B., Williams, J. G., and Arntzen, C. J. (1988) *EMBO J* **7**, 325-332
66. Pakrasi, H. B., Diner, B. A., Williams, J., and Arntzen, C. J. (1989) *Plant Cell* **1**, 591-597
67. Eaton-Rye, J. J., and Vermaas, W. (1991) *Plant Mol. Biol.* **17**, 1165-1177

FOOTNOTES

Acknowledgements
We would like to thank W.Vermaas, C. Funk, H. Pakrasi and J. Barber for providing us with deletion mutants and also L. A. Eichacker for the anti-CP47 antibody. The work was supported by the project MSM6007665808 of The Ministry of Education, Youth and Sports of the Czech

Republic, and by the Czech Academy of Sciences
Institutional Research Concept AV0Z50200510.

The abbreviations used are: BN-PAGE, blue native-polyacrylamide gel electrophoresis; CAB, chlorophyll *a/b* binding; Chl, chlorophyll; Cyt, cytochrome b_{559}; DBMIB, 2,5-dibromo-3-methyl-1,6-isopropyl-benzoquinone; DM, n-dodecyl-β-maltoside; ELIP, early light induced protein; HL, high-light; His tag, His_6epitope; HLIP, high-light induced protein; LHC, light-harvesting complex; Ni-NTA, nickel nitrilotriacetic acid; OHP, one-helix protein; PSI, photosystem I; PSII, photosystem II; RC, reaction center; RCC1, monomeric reaction center core; RC47, reaction center core lacking the inner antenna CP43; SCP, small Cab-like protein; SDS, sodium dodecyl sulfate; WT, wild type; 2D, two dimension.

FIGURE LEGENDS

Figure 1. Western blot detection of the His_6 epitope in thylakoids of ScpDHis/ΔScpD/PSI$^-$, uninduced ScpDHis/ΔScpD, and HL(high-light)-induced ScpDHis/ΔScpD mutants (lanes 1, 2 and 3, respectively).

Figure 2. Immunodetection of thylakoid membrane proteins from HL-induced ScpDHis/ΔScpD (A) and ScpDHis/ΔScpD/PSI$^-$/ΔCP47 (B) cells after separation of proteins by two-dimensional BN/SDS-PAGE. Thylakoid membrane proteins from HL-induced ScpDHis/ΔScpD and ScpDHis/ΔScpD/PSI$^-$/ΔCP47 cells were separated in the first dimension by BN-PAGE and in the second dimension by denaturing SDS-PAGE in a 12-20% linear gradient polyacrylamide gel, blotted onto PVDF membrane, and immunodetected using anti-His antibodies.

Figure 3. Autoradiogram of thylakoid membrane proteins from HL-induced WT (left) and ScpDHis/ΔScpD (right) of *Synechocystis* 6803 cells after separation of proteins by two-dimensional BN/SDS-PAGE. Thylakoid membrane proteins from both strains were pulse radiolabeled for 30 min, separated in the first dimension by BN-PAGE and in the second dimension by denaturing SDS-PAGE in a 12-20% linear gradient polyacrylamide gel, blotted onto PVDF membrane, and exposed to X-ray film. For the ScpDHis/ΔScpD autoradiogram, same membrane was used as in Fig. 2A.

Figure 4. Coomassie stain and immunodetection of D1 and ScpDHis in isolated PSII core complexes from ScpDHis/ΔScpD/PSI$^-$ cells after isolation of PSII by chromatography (lanes 1 and 2) or sucrose density-gradient centrifugation (dimeric and monomeric PSII; lanes 3 and 4) followed by separation by BN-PAGE. PSII from the ScpDHis/ΔScpD/PSI$^-$ strain was isolated by ion exchange chromatography or sucrose density-gradient centrifugation as described in 'Materials and Methods'. The isolated PSII protein complexes were further purified by BN-PAGE. The separated proteins were stained with Coomassie blue (lane 1) or blotted onto PVDF membrane and immunodetected using anti-His and anti-D1 antibodies (lanes 2, 3, and 4).

Figure 5. Immunodetection of thylakoid membrane proteins from ScpDHis/ΔScpD/PSI$^-$/ΔH (left) and ScpDHis/ΔScpD/PSI$^-$/ΔCyt (right) cells after separation of proteins by two-dimensional BN/SDS-PAGE. Thylakoid membrane proteins from the cells were separated in the first dimension by native BN-PAGE and in the second dimension by denaturing SDS-PAGE in a 12-20% linear gradient polyacrylamide gel and blotted onto PVDF membrane and immunodetected using anti-His and anti-CP47 antibodies.

Figure 6. Electron micrographs of dimeric PSII complexes labeled with Ni–NTA Nanogold and negatively stained with 0.75% uranyl acetate. Labeled particles in their top-view projection (circle) and their side-view projection (square) are indicated.

Figure 7. Single particle analysis of top-view and side-view projections of unlabeled (A–C) and ScpDHis PSII dimers labeled with Ni–NTA Nanogold (D-F). The projections are presented as facing from the

lumenal side of the thylakoid membrane and the numbers of summed images are: 645 (A), 580 (B), 175 (C), 152 (D), 185 (E), and 84 (F).

Figure 8. Top-view projection map of the ScpDHis PSII core complex labeled with Ni–NTA Nanogold overlaid with the cyanobacterial X-ray model of the dimeric PSII core complex resolved at 3.5 Å resolution (49), Protein Data Bank accession number 1S5L. Carbon atoms and amino acid side chains of the major PSII subunits are representated in separate colors: CP47 (green), CP43 (blue), D1 (orange), D2 (yellow) and cytochrome b_{559} (violet). Single transmembrane helices assigned to low molecular weight PSII subunits are represented as solid ribbons in gray color except for PsbH subunit (in red). Heteroatoms and extrinsic proteins are not shown. The Ni–NTA Nanogold label is observed on both sides of the complex (black arrows). Deduced location of the ScpD subunit(s) within the dimeric PSII core complex is indicated by dashed area in the vicinity of the CP47 and PsbH subunit.

Table 1.

Synechocystis 6803 mutants

Strains	Ref.
WT	(64)
ΔCyt	(65,66)
ΔCP47	(67)
ΔH	(50)
ScpDHis/ΔScpD	This study
ScpDHis/ΔScpD/PSI$^-$	This study
ScpDHis/ΔScpD /PSI$^-$/ΔCyt	This study
ScpDHis/ΔScpD /PSI$^-$/ΔCP47	This study
ScpDHis/ΔScpD/PSI$^-$/ΔH	This study

Figure 1.

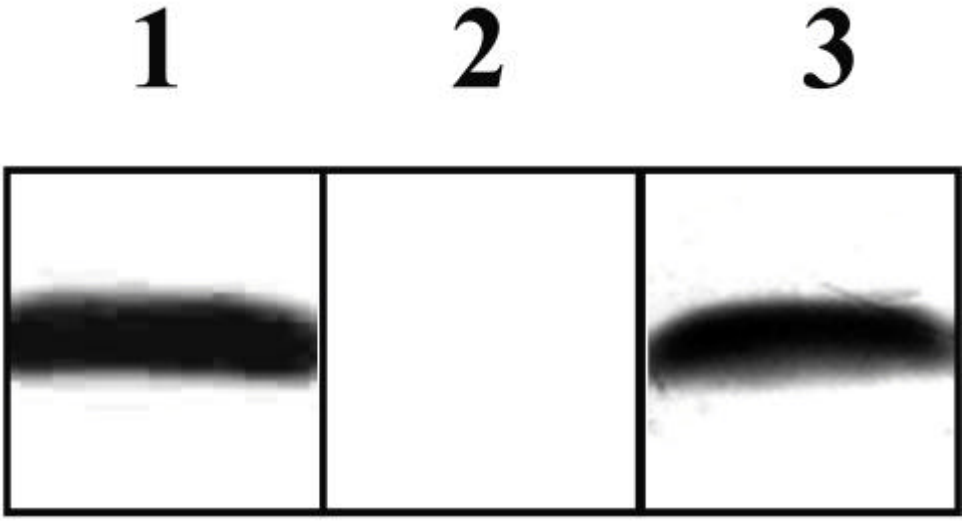

Figure 2.

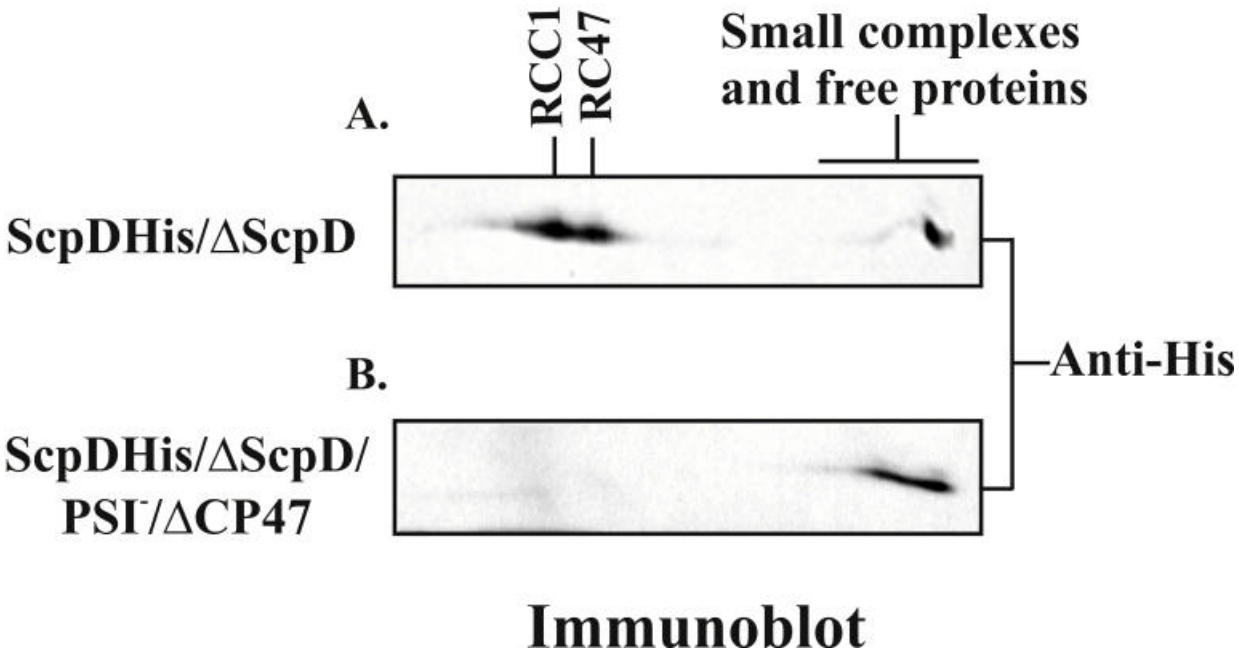

Immunoblot

Figure 3.

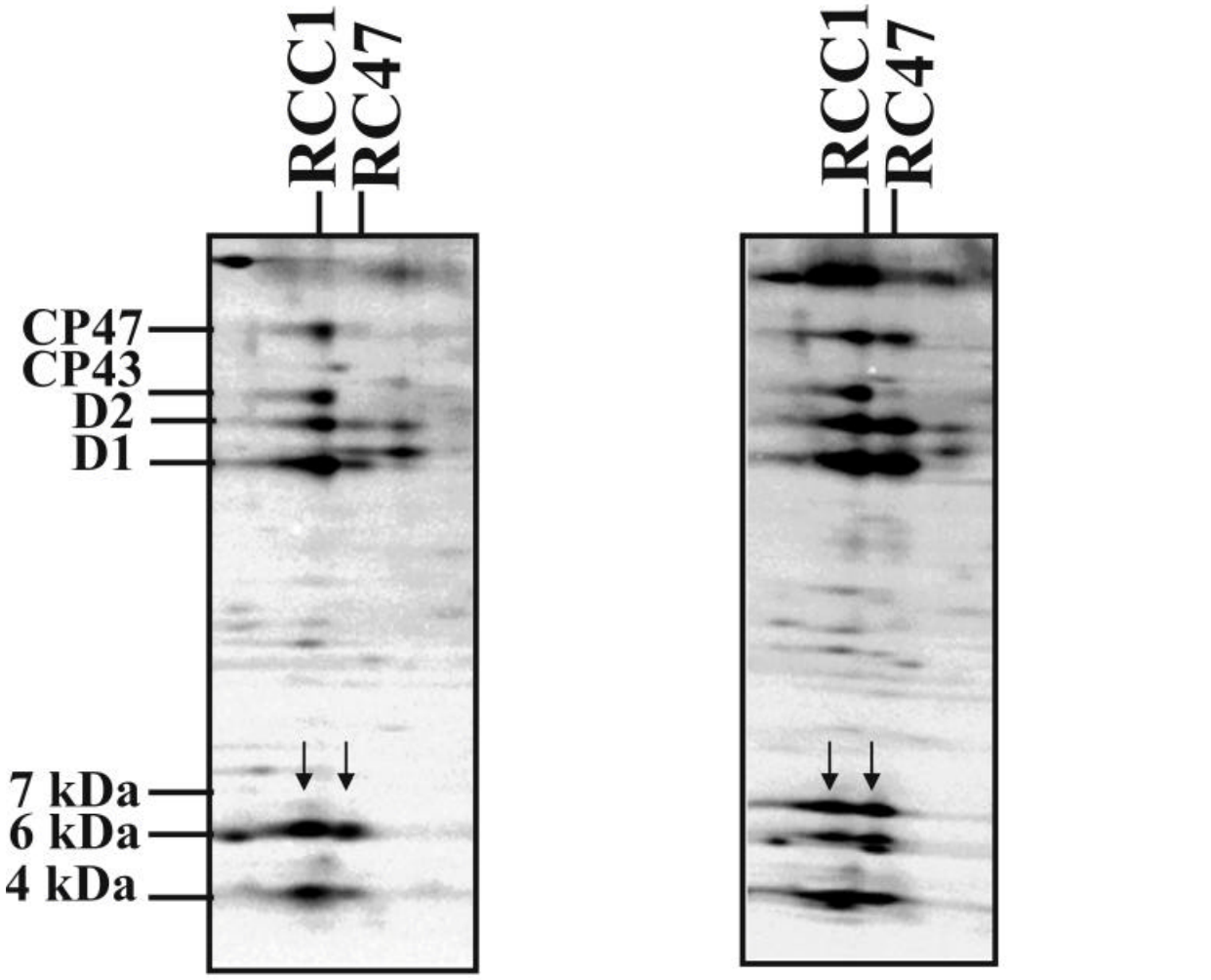

Autoradiograms

Figure 4.

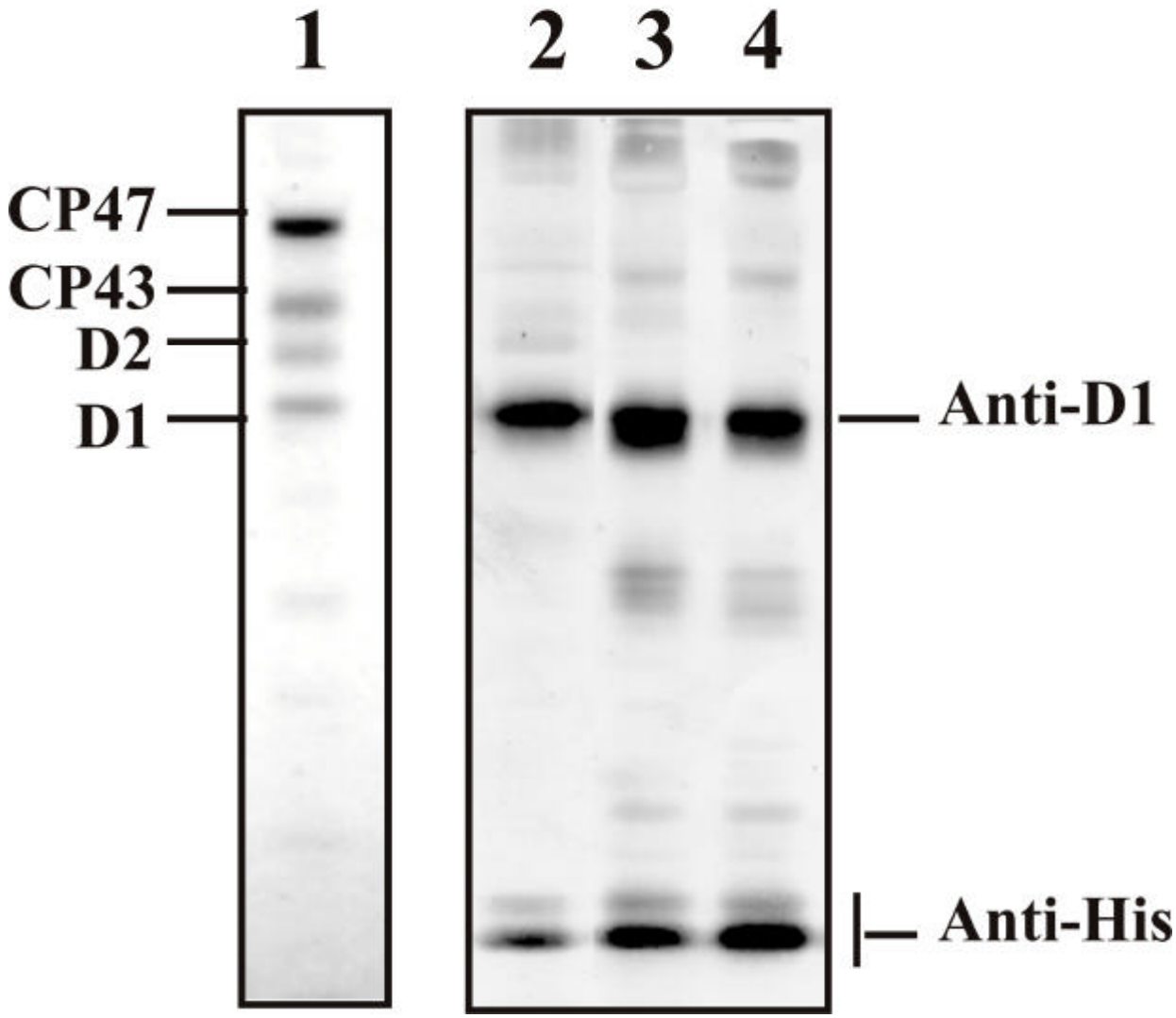

Figure 5.

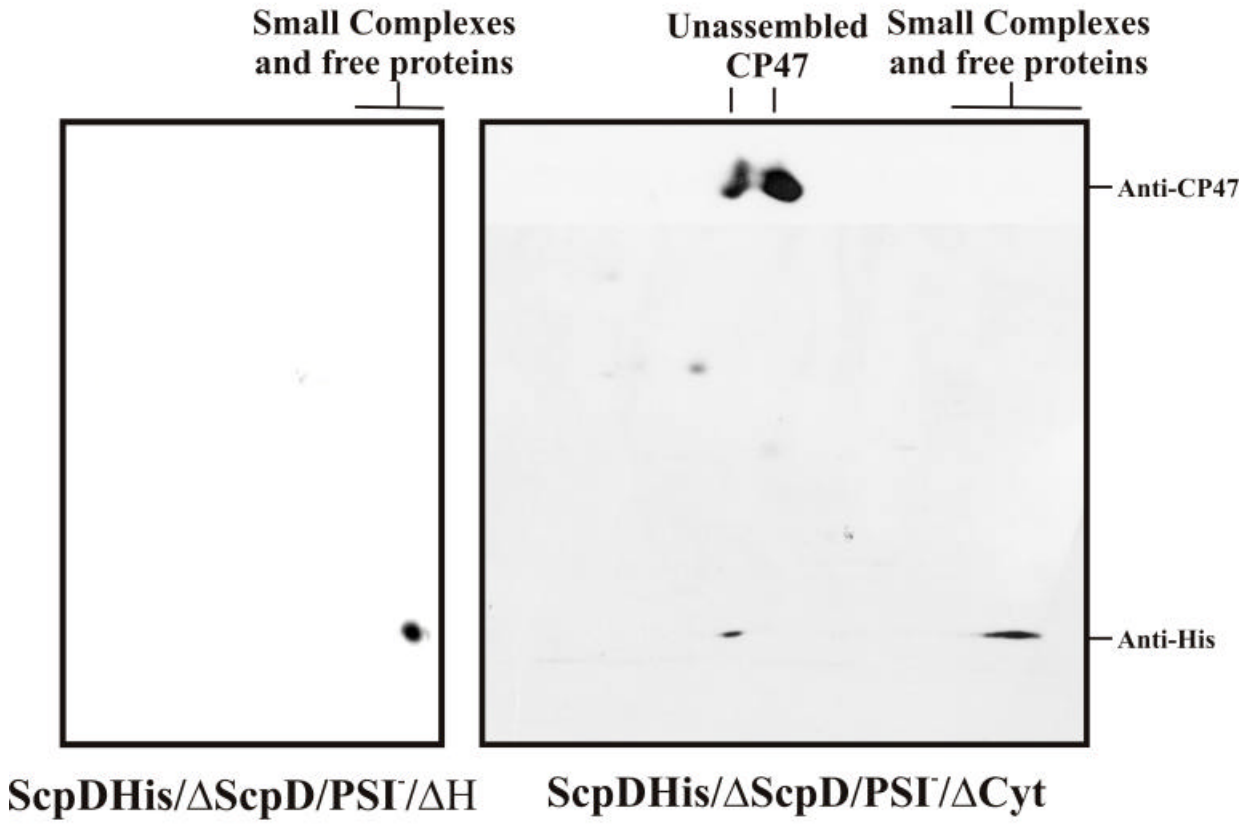

Figure 6.

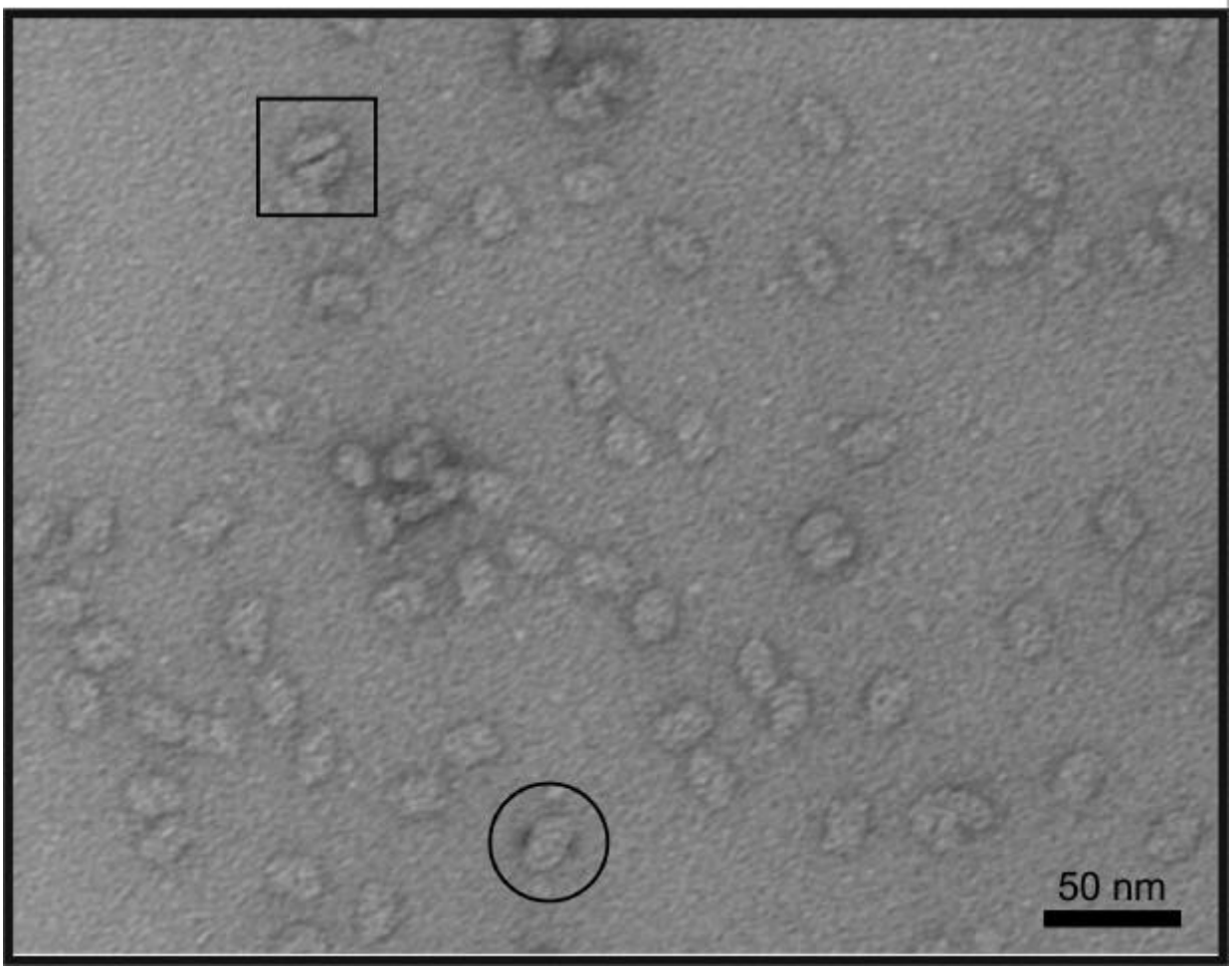

Figure 7.

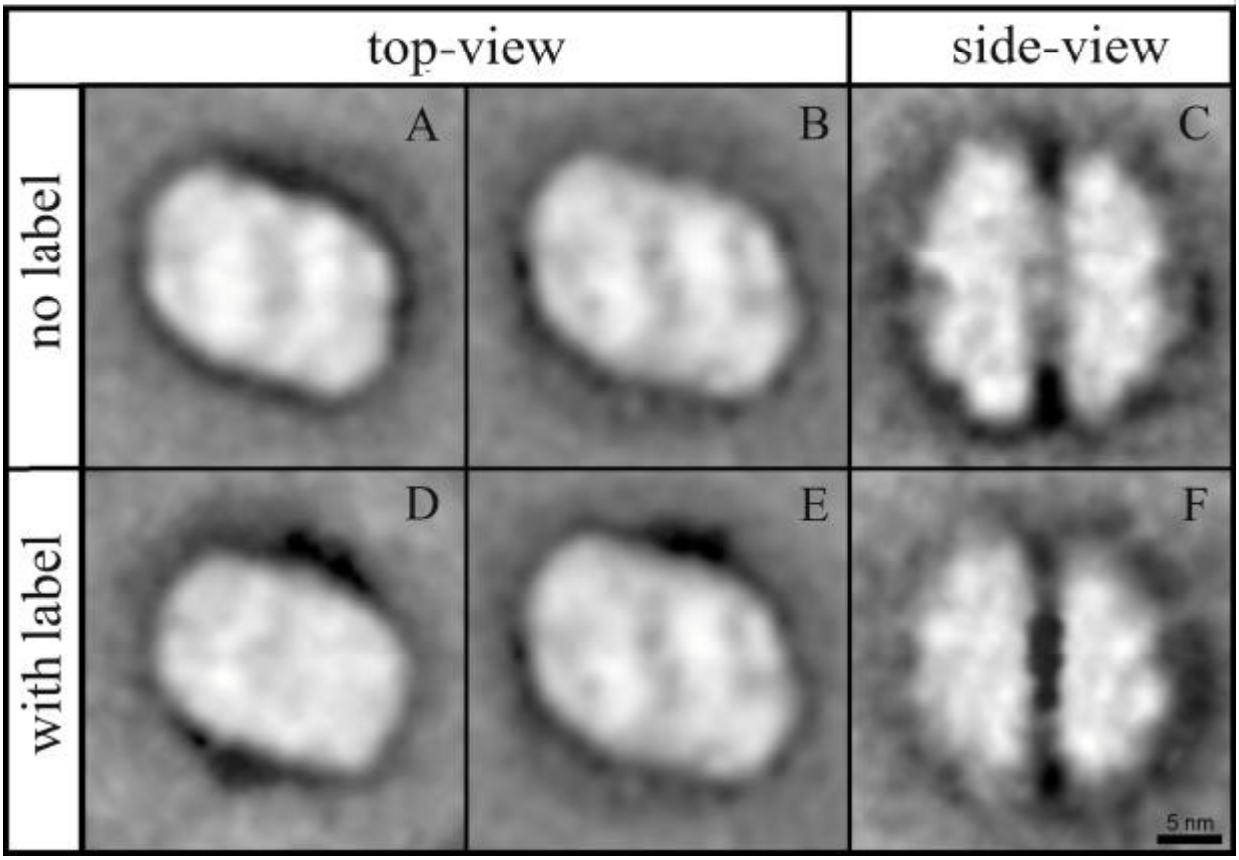

Figure 8.